Chemical Science

Check for updates

All publication charges for this article have been paid for by the Royal Society of Chemistry

Asymmetric intramolecular reductive coupling of bisimines templated by chiral diborons†

Tian Chen,‡[a] Hao-Yang Wang,‡[c] Ronghua Xu,[b] Guangqing Xu,[b] He Yang,*[b] Jiangtao Sun, [ID] *[a] Lung Wa Chung [ID] *[c] and Wenjun Tang [ID] *[ad]

An asymmetric intramolecular reductive coupling of bisimines has been accomplished for the first time under mild conditions with bis((+)-pinanediolato)diboron as the template, providing the unprecedented chiral dihydrophenanthrene-9,10-*cis*-diamines in high yields and excellent enantioselectivities. The chiral exocyclic *cis*-diamine products have served as effective chiral ligands for asymmetric catalysis. A DFT study highlights the crucial roles of the uncommon twisted-boat pathway (instead of the common chair type) and the steric effect in exclusively forming the *cis*-diamines and achieving high enantioselectivity. This reductive coupling protocol represents a significant expansion of the diboron-promoted [3,3]-sigmatropic rearrangement.

Introduction

Chiral exocyclic vicinal *cis*-diamines[1] belong to a unique class of chiral vicinal diamines that are found in the structures of a number of biologically important natural products and therapeutic agents (Fig. 1a). For example, biotin,[2] containing a chiral *cis*-diamine substructure on a tetrahydrothiofuran ring, is involved in a wide range of metabolic processes as one of the B vitamins; edoxaban,[3] a factor Xa inhibitor used as an anticoagulant medication, possesses a chiral cyclohexane *cis*-diamine scaffold; saxitoxin,[4] bearing a *cis*-diamine structure on a cyclic guanidine, is a neurotoxin that acts as a sodium channel blocker. In addition, enantiomerically pure exocyclic vicinal *cis*-diamines serve as conformationally rigid and sterically bulky backbones for transition-metal catalysts in asymmetric catalysis.[5] However, despite the significant progress in the synthesis of chiral acyclic vicinal diamines[6] and exocyclic *trans*-diamines,[7] the construction of chiral exocyclic vicinal *cis*-diamines, mainly

based on a cyclohexane skeleton, remains a significant challenge.[8] The current reported methods suffered from either lengthy synthetic sequences[8d] or low diastereo- and/or enantioselectivities.

We have recently developed an efficient method for the synthesis of chiral vicinal diamines through asymmetric intermolecular reductive homocoupling of imines templated by chiral diborons (Fig. 1b).[9] The featured diboron-promoted [3,3]-sigmatropic rearrangement has enabled the single-step synthesis of chiral tetrahydro-bisisoquinolines, bis(cyclic amine)s, acyclic vicinal disubstituted diamines, and acyclic vicinal tetrasubstituted diamines in excellent yields, diastereoselectivities, and enantioselectivities. By using bisaldimines as starting materials, polymeric chiral diamines were synthesized in a highly stereoselective fashion with M_n ranging from 5000 to 14 000.[9d] In contrast, efficient asymmetric intramolecular reductive coupling of bisimines has not been realized. Such transformation would lead to chiral exocyclic vicinal diamines in a step-economic fashion.

There are several challenges for such an unprecedented transformation: (1) chemoselectivity: how to inhibit the intermolecular polymerization and enforce the intramolecular cyclization? (2) Diastereoselectivity: would the intramolecular diboron-promoted [3,3]-sigmatropic rearrangement proceed through a chair-like six-membered transition state to form a *trans*-diamine or a *cis*-diamine? (3) Enantioselectivity: can a chiral exocyclic diamine be constructed in a single step from a readily available starting material? In this study, we have successfully addressed the above challenges by judicious selection of bisimine substrates and chiral diborons, and accomplished the first and asymmetric intramolecular reductive coupling of bisimines (Fig. 1c). The coupling protocol has enabled one-step synthesis of unprecedented

[a] *Jiangsu Key Laboratory of Advanced Catalytic Materials & Technology, School of Petrochemical Engineering, Changzhou University, 1 Gehu Road, Changzhou 213164, China. E-mail: jtsun@cczu.edu.cn*

[b] *State Key Laboratory of Chemical Biology, Shanghai Institute of Organic Chemistry, University of Chinese Academy of Sciences, 345 Ling Ling Road, Shanghai 200032, China. E-mail: yanghe@sioc.ac.cn; tangwenjun@sioc.ac.cn*

[c] *Shenzhen Grubbs Institute, Department of Chemistry and Guangdong Provincial Key Laboratory of Catalysis, Southern University of Science and Technology, Shenzhen 518055, China. E-mail: oscarchung@sustech.edu.cn*

[d] *School of Chemistry and Materials Science, Hangzhou Institute for Advanced Study, University of Chinese Academy of Sciences, 1 Sub-lane Xiangshan, Hangzhou 310024, China*

‡ These authors contributed equally to this work.

Fig. 1 Chiral *cis*-diamines and their enantioselective syntheses by intramolecular asymmetric reductive coupling of bisimine. (a) The prevalence of chiral *cis*-diamines. (b) Intermolecular asymmetric reductive coupling of imines templated by chiral diborons. (c) This study on intramolecular asymmetric reductive coupling of imines.
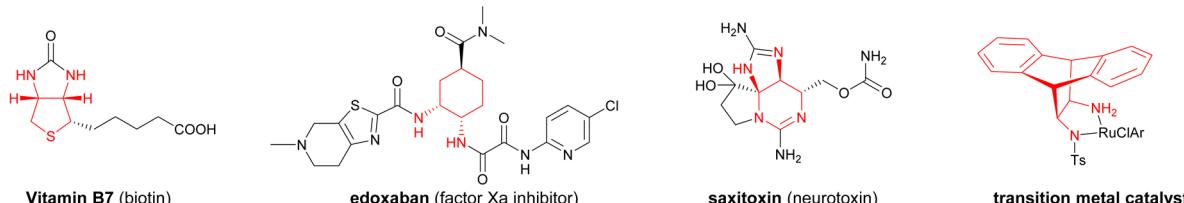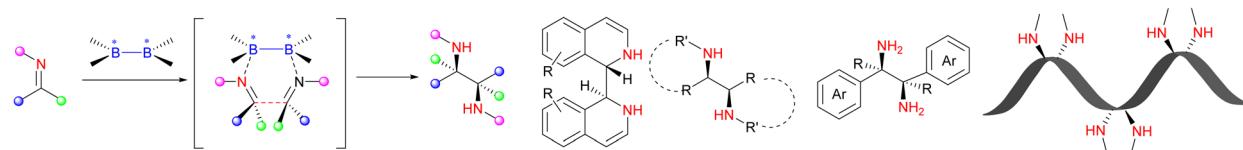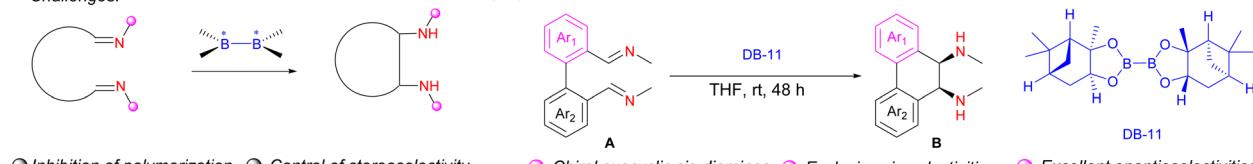
dihydrophenanthrene-9,10-*cis*-diamines and provided excellent yields, exclusive *cis* selectivities, and almost perfect enantiose-lectivities, by employing chiral bis(pinanediolato)diboron as the template.

Results and discussion

At the outset of our study, the feasibility of intramolecular reductive coupling of bisimines was investigated with the hexane-1,6-diimine substrate (**1a**), which was *in situ* prepared from adipaldehyde and ammonia (Fig. 2a). Treatment of **1a** with (Bpin)$_2$ at rt provided a mixture of polyamines without detection of intramolecular cyclization product **2a**. We assumed that the intermolecular coupling was more favorable than the intra-molecular coupling in the case of **1a**. A structurally more rigid diimine **1b** could be more suitable for intramolecular coupling. Thus, compound **1b** was prepared *in situ* from [1,1′-biphenyl]-2,2′-dicarbaldehyde and ammonia and treated with (Bpin)$_2$ at rt. Indeed, a trace amount of the intramolecular coupling product **2b** was formed according to LC-MS, and the major isolated product was 5-hydroxy-5*H*-dibenzo[*c,e*]azepin (**2b′**).[10] These results showed that the intramolecular coupling of bisimine could be accomplished by inhibiting the polymerization process and other side reactions, including hydrolysis and formation of a stable dibenzo[*c,e*]azepin derivative, by employ-ing substrates with increased rigidity and steric hindrance. Pleasingly, the efficiency of the intramolecular coupling was significantly enhanced when *N*-substituents were introduced into the substrate. Thus, **1c** was treated with (Bpin)$_2$ under similar conditions, and the resulting cyclization *cis*-diamine

product **2c** was formed in 80% yield, whose relative configura-tion was confirmed by the X-ray crystal structure of its urea derivative **3c** (Fig. 2b).[11] Notably, the unexpected formation of *cis*-diamine **2c** was intriguing since no *meso* products were formed in our previous reports on various intermolecular reductive homocouplings of imines.[9] Despite the symmetry of *cis*-diamine **2c**, we proposed that a chiral *cis*-diamine would be constructed for the first time if an unsymmetrical bisimine based on the [1,1′-biphenyl]-2,2′-dicarbaldehyde skeleton was employed, and an effective chiral diboron template could be discovered. Hence, 3-methoxy-[1,1′-biphenyl]-2,2′-dicarbalde-hyde (**4a**) was treated with MeNH$_2$·HCl and triethylamine *in situ* to form bisimine **5a**, which was then treated with chiral dibor-ons in THF at rt for 48 h (Fig. 2c). Encouragingly, the chiral diboron with four phenyl substituents **DB1** provided **6a** in 85% yield and 22% ee. This proof-of-concept result demonstrated the feasibility of forming **6a** in high enantioselectivity by screening various chiral diborons. While **DB2** with bromo substituents showed no reactivity, **DB3** with six phenyl substituents led to **6a** in 84% yield and 55% ee. Further modi-fications of substituents on the aryl groups in **DB4-10** all provided good yields, but with moderate enantioselectivities. Finally, employment of chiral bis(pinanediolato)diboron **DB11** led to the formation of **6a** in 90% yield and 99% ee. Further solvent screening showed that the cyclization proceeded with similarly high enantioselectivities in various solvents, indi-cating the robustness of the transformation (see the ESI† for more details).

The substrate scope of intramolecular reductive coupling was studied. As can be seen from Table 1, unsymmetrical [1,1′-
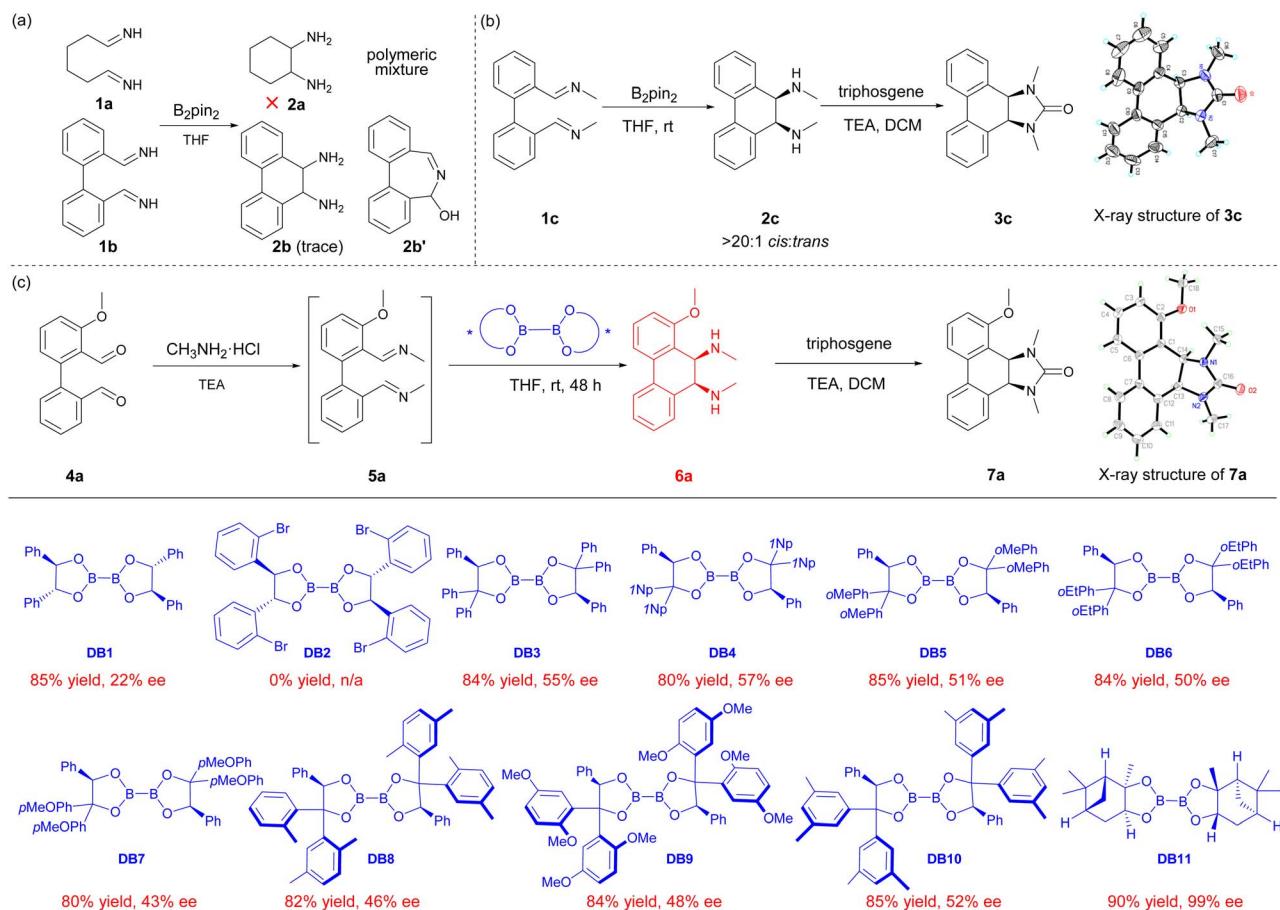
Fig. 2 Asymmetric intramolecular reductive coupling of bisimine **5a** templated by various chiral diborons. (a) Attempts on diboron templated intramolecular reductive coupling of bisimines. (b) Formation of *cis*-diamine by diboron templated intramolecular reductive coupling. (c) The development of asymmetric intramolecular reductive coupling protocol.

biphenyl]-2,2′-bisimine substrates with various 3-substituents were employed, providing chiral dihydrophenanthrene-9,10-*cis*-diamines **6a–h** in moderate to high yields. While most products **6d–g** were formed in almost perfect enantioselectivities regardless of their electronic properties, the small-size fluoro-substituted product **6c** was obtained in 56% ee, indicating that the size of the substituent might be influential to the enantioselectivity. In addition, product **6h** with a dioxolane ring was less selective (75% ee). The presence of 3-substitution (*ortho*-substitution) appeared to be crucial for the enantioselectivity, as substrates with 4- or 5-methoxy substituents provided very low enantioselectivities (see the ESI† for more details).

By fixing the upper aryl ring with a methoxy substituent at the 3′ position, the substitution effect on the lower aryl ring was studied. The excellent enantioselectivities (91–99% ee) obtained for **6i–u** demonstrated that the reaction was compatible with various substituents at 3′, 4′, and 5′ positions regardless of their electronic properties. It was interesting that products **6o** and **6p** with *ortho*-substituents on both upper and lower rings were obtained in excellent ee's. The synthesis of product **6v** with a thiophene ring was extremely enantioselective (99% ee). A substrate with a naphthalene upper ring was also compatible,

forming **6w** in 88% yield and 99% ee. Surprisingly, product **6x** with a dioxolane ring at both 4′ and 5′ positions was afforded in a low ee (30%). Substrates with multiple substituents on the upper aryl ring were also suitable. While the optical purity of product **6y** with *ortho*-fluoro substituent was inferior (47% ee), product **6z** with *ortho*-bromo substituent was obtained in 99% ee. The intramolecular reductive coupling was not limited to *N*-methyl substituents. A substrate with *N*-ethyl substituents was also compatible, leading to **6ab** in 36% yield and 71% ee. Finally, substrates with 3-aryl substituents were employed, forming a series of *ortho*-aryl dihydrophenanthrene-9,10-*cis*-diamines **6ac–aj** in good yields (53–98%) and excellent enantioselectivities (95–99% ee).

The exclusive formation of uncommon *cis*-diamine products and excellent enantioselectivities from the intramolecular reductive coupling called for a plausible mechanistic rationale. To gain insights into the reaction mechanism and the origin of the enantioselectivity, a systematic DFT study (SMD M06-2X-D3/def2-TZVP//SMD M06-2X-D3/BS1 method mainly) was first conducted by using the chiral diboron agent **DB11** and the bisimine substrate **5e** (R=Br; Fig. 3).[11] Compared with our previous studies on the intermolecular coupling systems,[9a,c,11e] our current computational results reveal a distinct feature for

Table 1 Asymmetric intramolecular reductive coupling of bisimine **5** templated by chiral diboron **DB11** [a]

6a	**6b**	**6c**	**6d**	**6e**	**6f**	**6g**
90% yield, 99% ee	71% yield, 95% ee	87% yield, 56% ee	98% yield, 98% ee	88% yield, 99% ee	73% yield, 99% ee	85% yield, 99% ee

6h	**6i**	**6j**	**6k**	**6l**	**6m**	**6n**
59% yield, 75% ee	43% yield, 96% ee	95% yield, 91% ee	60% yield, 99% ee	92% yield, 99% ee	85% yield, 97% ee	39% yield, 96% ee

6o	**6p**	**6q**	**6r**	**6s**	**6t**	**6u**
53% yield, 99% ee	55% yield, 90% ee	75% yield, 94% ee	77% yield, 99% ee	57% yield, 98% ee	60% yield, 94% ee	61% yield, 94% ee

6v	**6w**	**6x**	**6y**	**6z**	**6ab**	**6ac**
53% yield, 99% ee	88% yield, 99% ee	86% yield, 30% ee	79% yield, 47% ee	76% yield, 99% ee	36% yield, 71% ee	87% yield, 99% ee

6ad	**6ae**	**6af**	**6ag**	**6ah**	**6ai**	**6aj**
80% yield, 99% ee	98% yield, 95% ee	97% yield, 98% ee	53% yield, 99% ee	85% yield, 97% ee	70% yield, 99% ee	52% yield, 99% ee

[a] Unless otherwise specified, the reactions were carried out at rt with **5a–aj** (0.2 mmol, 1.0 equiv.), **DB11** (0.2 mmol, 1.0 equiv.) in THF (10 mL) for 48 h. Isolated yields. The ee values were determined by chiral HPLC analysis.

this intramolecular coupling of bisimines. This intramolecular coupling adopts uncommon twisted boat transition states during the [3,3]-sigmatropic rearrangement to afford the synthetically challenging chiral vicinal *cis*-diamines, due to the ring strain of the bisimine tether (Fig. 3b, S2 and S3†). In contrast, the previous intermolecular coupling systems follow
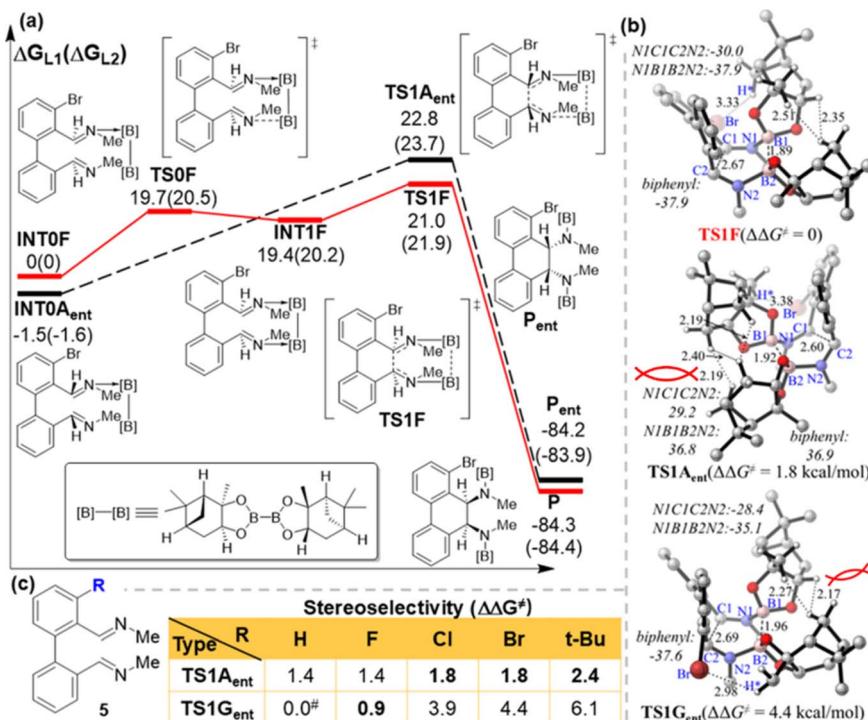
Fig. 3 (a) Calculated Gibbs free energy profile of the reaction of **DB11** with **5e** (R=Br) at the SMD M06-2X-D3/BS1 (L1) and SMD M06-2X-D3/def2-TZVP//SMD M06-2X-D3/BS1 (L2) levels (see ref. 11a). (b) Computed structures and key geometric parameters (distances in Å and dihedrals in italics and degrees) of the three key coupling transition states with their relative Gibbs free energies. Unimportant H atoms were omitted for clarity. (c) The effect of R substituents on the relative Gibbs free energy (in kcal mol^{-1}) of the two key transition states to form the minor product with respect to their corresponding lowest-energy **TS1F** forms leading to the major product at the SMD M06-2X-D3/def2-TZVP//SMD M06-2X-D3/BS1 level. #**TS1G$_{ent}$-H** has the same geometry as **TS1F-H**.

the common chair-type pathway.[9a,c,11e] A total of 16 conformers for the coupling transition states (TSs) (Tables S8 and S10, Fig. S2 and S3†) were located for **5e** through our comprehensive conformational search, with eight of them yielding the major product (**P**) and the others yielding the enantiomer product (**P$_{ent}$**). As shown in Fig. 3a, the most favorable **TS1F** leading to the desired coupling product (**P**) was computed to be lower in free energy than that giving the minor product **P$_{ent}$** via **TS1A$_{ent}$** by 1.8 kcal mol^{-1}. This result qualitatively explains the observed stereochemistry. The similar free energy difference ($\Delta\Delta G^{\neq}$) is also supported by a few different common computational methods (Tables S9 and S11†).

Additional calculations were conducted to examine the size effect of R (F, Cl, Br or H) on the stereoselectivity (Fig. 3c, S4 and Tables S12–S17†). Likewise, the same favorable coupling TSs (**TS1F-Cl** and **TS1A$_{ent}$-Cl**) and free energy difference ($\Delta\Delta G^{\neq}$ ~1.8 kcal mol^{-1}) for **5d** (R=Cl) were also found. In contrast, **5c** (R= F) adopts another and lower-energy conformer for the minor-coupling TS (**TS1G$_{ent}$-F**), which reduces the free energy difference between the two stereo-determining coupling TSs ($\Delta\Delta G^{\neq}$) to ~0.9 kcal mol^{-1} only. To examine the steric effect of R on the energetics of the three key coupling TSs, tBu was employed and found to further increase the free energy difference ($\Delta\Delta G^{\neq}$ ~2.4–6.1 kcal mol^{-1} vs. 1.8–4.4 kcal mol^{-1} for R=Br; Table S18†). Overall, these computational results are in qualitative agreement with the experimental observation, highlighting the

essential role of the steric effect of the R substituent in controlling stereoselectivity (particularly for the **TS1G$_{ent}$** type TSs).

As shown in Fig. 3b and S4,† the major coupling TSs (**TS1F**, **TS1F-Cl** and **TS1F-F**) can avoid steric congestion between the halogen substituent and diboron as well as minimize H–H repulsion inside the diboron part (especially on the methylene bridge; see Fig. S6†). In contrast, the minor coupling TSs (e.g. **TS1A$_{ent}$** and **TS1G$_{ent}$**) suffer from more steric hindrance between R and the diboron as well as more severe H–H repulsion in the diboron part. Generally, such steric crowdedness slightly increases the dihedral angle along the biphenyl C–C single bond (diminishing delocalization) and decreases the dihedral angles of the boat-shaped [3,3]-sigmatropic rearrangement TS structure (Table S19†). The **TS1G$_{ent}$** and **TS1F** form TSs adopt the essentially same conformation except for the substituent positioned in different arene rings. For a very small substituent (R=F or H), the **TS1G$_{ent}$** form TSs are more energetically favorable to form the minor product than the **TS1A$_{ent}$** form TSs and lead to a smaller free energy difference with the **TS1F** form TSs. However, the **TS1G$_{ent}$** form TSs become unfavorable than the **TS1A$_{ent}$** and **TS1F** form TSs with a larger R (R=Cl or Br), since the R substituent has the closest contact with the diboron in the **TS1G$_{ent}$** form TSs and experiences more steric repulsion. In addition, the most favorable **TS1F** type TSs have a lesser B–B bond elongation than the other two minor-
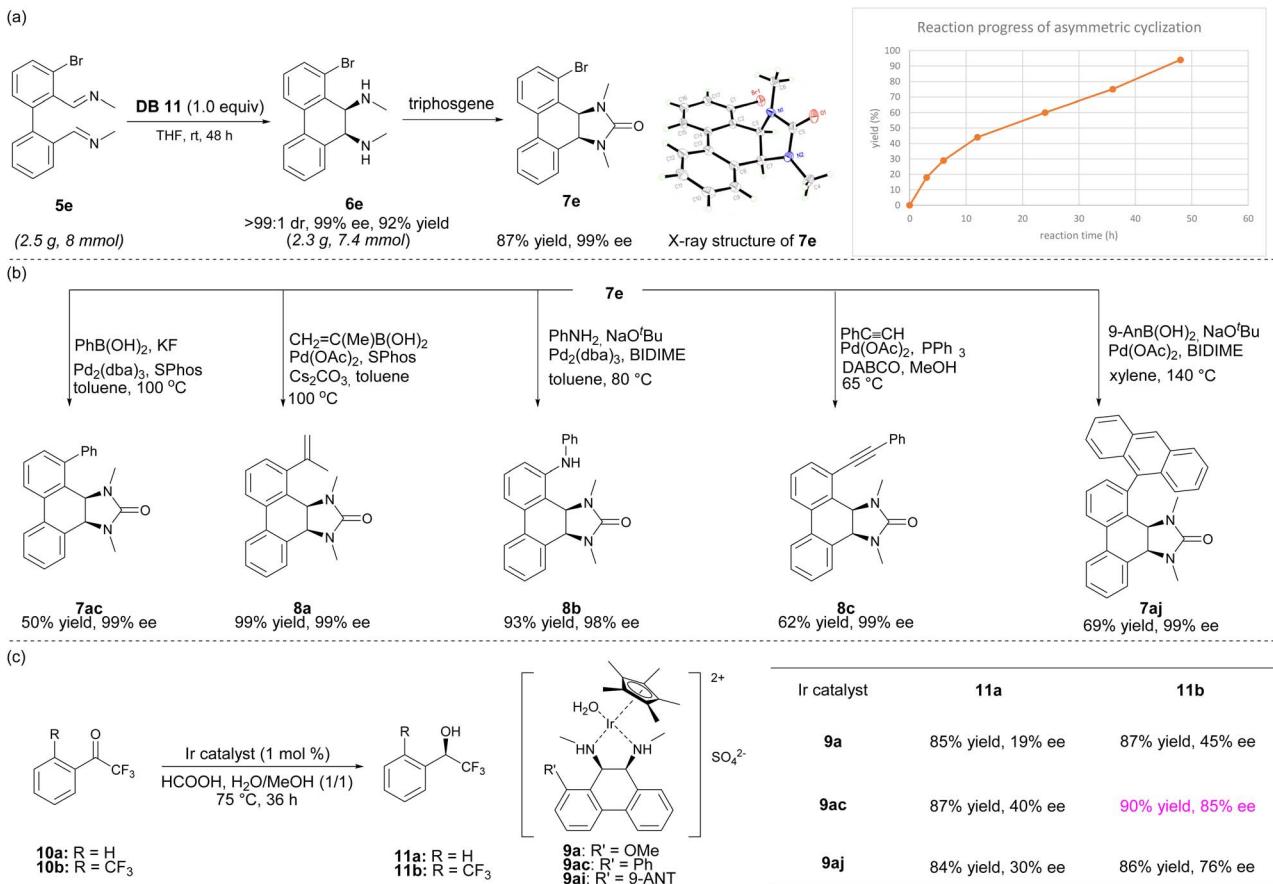
Scheme 1 Derivatization and catalytic applications of chiral *cis*-diamines. (a) Gram scale reaction and kinetic profile. (b) Transformation of coupling product. (c) Utility of chiral *cis*-diamine product in asymmetric transfer hydrogenation.

type TSs. Distortion/interaction analysis[12] further revealed that the **TS1F** type TSs have smaller distortion energy than the two types of minor TSs ($\Delta\Delta E_{dist}$ = 2.7–4.0 kcal mol^{-1} for R=F and 3.3–9.1 kcal mol^{-1} for R=Br; Table S20†), which plays a vital role in the stereoselectivity. Local distortion analysis[13] on the 10-atom diboron core part also gave comparable relative distortion energies for these key TSs ($\Delta\Delta E_{dist}$ = 1.5–5.3 kcal mol^{-1} for R=Br; Fig. S5†).

To demonstrate the practicality of this transformation, the reductive cyclization of **5e** was performed in THF at rt for 48 h in the presence of **DB11** at a 2.5 gram scale and product **6e** was obtained in 92% yield and 99% ee as a single diastereomer (Scheme 1a). Treatment of **6e** with triphosgene and TEA provided **7e**, whose absolute stereochemistry was confirmed by its X-ray crystal structure. The yields from **5e** to **6e** were monitored by NMR studies, and the intramolecular reductive coupling was found to be a much slower process, in contrast to the previously reported intermolecular homocoupling of isoquinolines.[9a] The chiral bromo-substituted product **7e** was a versatile intermediate for further derivatization (Scheme 1b). The Suzuki–Miyaura coupling of **7e** with phenylboronic acid or prop-1-en-2-ylboronic acid catalyzed by Pd/SPhos afforded products **7ac** and **8a** in 50% yield and 99% yield, respectively,

without erosion of enantiomeric purities (99% ee). Moreover, the Suzuki–Miyaura coupling of **7e** with 9-anthrylboronic acid proceeded with Pd(OAc)$_2$ and BIDIME as the catalyst system to give **7aj** in 69% yields. A Buchwald–Hartwig coupling of **7e** with aniline catalyzed by Pd/BIDIME delivered **8b** in 93% yield. In addition, Sonogashira coupling of **7e** with phenylacetylene led to **8c** in 62% yield and 99% ee.

The conformationally rigid chiral *cis*-diamine products were suitable ligands for asymmetric catalysis. We envisioned that its η^5 iridium complex could be suitable for asymmetric transfer hydrogenation.[9d,14] Therefore, iridium complexes **9a**, **9ac**, and **9aj** were prepared and applied to the asymmetric transfer hydrogenation of trifluoroacetophenones **10a** and **10b** (Scheme 1c). All reductions were found to be enantioselective. Notably, the asymmetric transfer hydrogenation of **10b** with catalyst **9ac** provided **11b** in 90% yield and 85% ee, demonstrating the effectiveness of these chiral *cis*-diamines as chiral ligands in asymmetric catalysis.

Conclusions

In summary, we have developed an asymmetric intramolecular reductive coupling of bisimines under mild conditions using

chiral bis(pinanediolato)diboron as the template, providing the unprecedented chiral dihydrophenanthrene-9,10-cis-diamines in high yields and excellent enantioselectivities. Our systematic computational investigation has revealed the vital roles of a less common twisted-boat pathway (rather than the common chair pathway) and steric effect in exclusively forming the cis-diamines and achieving high enantioselectivity for this first intramolecular reductive coupling. The chiral exocyclic cis-diamine products are effective ligands for asymmetric catalytic reactions. This method signifies the broad scope of the diboron-promoted [3,3]-sigmatropic rearrangement and enriches the chemistry of chiral vicinal cis-diamines.

Data availability

The ESI† is available and includes full experimental details, synthesis protocols, characterization data, and spectroscopic details. CCDC 2428416 (compound **3c**), 2428418 (compound **7a**), and 2428420 (compound **7e**) contain the supplementary crystallographic data for this paper. These data can be obtained free of charge via **https://www.ccdc.ca-m.ac.uk/data_request/cif**, or by emailing data_request@ccdc.cam.ac.uk, or by contacting the Cambridge Crystallographic Data Centre, 12 Union Road, Cambridge CB2 1EZ, UK; fax: +44 1223 336033.

Author contributions

W. T., G. X. and H. Y. conceptualised the work. T. C., R. X. and H. Y. conducted experiments. H.-Y. W. and L. W. C. performed DFT calculations. The manuscript was written through contributions of all authors. W. T., L. W. C., J. S. and H. Y. supervised the work, secured funding, edited and finalised the manuscript.

Conflicts of interest

The authors declare no competing financial interest.

Acknowledgements

Notes and references

1 (a) D. Lucet, T. Le Gall and C. Mioskowski, Angew. Chem., Int. Ed., 1998, **37**, 2580–2627; (b) F. Foubelo, C. Nájera, M. G. Retamosa, J. M. Sansano and M. Yus, Chem. Soc. Rev., 2024, **53**, 7983–8085; (c) S. R. S. S. Kotti, C. Timmons and G. Li, Chem. Boil. Drug. Des., 2006, **67**, 101–114; (d) Z. L. Tao and S. E. Denmark, Synthesis, 2021, **53**, 3951–3962; (e) A. K. Weber, J. Schachtner, R. Fichtler, T. M. Leermann, J. M. Neudörfl and A. J. von. Wangelin, Org. Biomol. Chem., 2014, **12**, 5267–5277; (f) B. Yang, A. Yu and Y. Wang, ChemCatChem, 2023, **15**, e202300141.

2 (a) A. Marquet, Pure Appl. Chem., 1993, **65**, 1249–1252; (b) C. A. Perry and T. A. Butterick, Adv. Nutr., 2024, **15**, 100251.

3 (a) M. Poulakos, J. N. Walker, U. Baig, T. David and Am. J. Health, Syst Pharm., 2017, **74**, 117–129; (b) G. E. Raskob, N. van. Es, P. Verhamme, M. Carrier, M. D. Nisio, D. Garcia, M. A. Grosso, A. K. Kakkar, M. J. Kovacs, M. F. Mercuri, G. Meyer, A. Segers, M. Shi, T.-F. Wang, E. Yeo, G. Zhang, J. I. Zwicker, J. I. Weitz and H. R. Büller, N. Engl. J. Med., 2018, **378**, 615–624.

4 (a) V. Pratheepa and V. Vasconcelos, Mini. Rev. Med. Chem., 2017, **17**, 320–327; (b) A. P. Thottumkara, W. H. Parsons and J. D. Bois, Angew. Chem., Int. Ed., 2014, **53**, 5760–5784; (c) L. E. Llewellyn, Nat. Prod. Rep., 2006, **23**, 200–222; (d) K. D. Cusick and G. S. Sayler, Mar. Drugs, 2013, **11**, 991–1018.

5 (a) H. Zhou, Y. Z. Geng and S. W. Yan, Acta Phys. Sin., 2023, **72**, 068702; (b) T. A. Davis and J. N. Johnston, Chem. Sci., 2011, **2**, 1076–1079.

6 (a) Y.-W. Zhong, K. Izumi, M.-H. Xu and G.-Q. Lin, Org. Lett., 2004, **6**, 4747–4750; (b) E. P. Vanable, J. L. Kennemur, L. A. Joyce, R. T. Ruck, D. M. Schultz and K. L. Hull, J. Am. Chem. Soc., 2019, **141**, 739–742; (c) J. Chen, X. Gong, J. Li, Y. Li, J. Ma, C. Hou, G. Zhao, W. Yuan and B. Zhao, Science, 2018, **360**, 1438–1442; (d) P. Zhou, X. Shao and S. J. Malcolmson, J. Am. Chem. Soc., 2021, **143**, 13999–14008; (e) Y. Chen, Y. Pan, Y. M. He and Q. H. Fan, Angew. Chem., Int. Ed., 2019, **58**, 16831–16834; (f) L. Yu and P. Somfai, Angew. Chem., Int. Ed., 2019, **58**, 8551–8555; (g) Z. Tao, B. B. Gilbert and S. E. Denmark, J. Am. Chem. Soc., 2019, **141**, 19161–19170; (h) S. Roland, P. Mangeney and A. Alexakis, Synthesis, 1999, **2**, 228–230; (i) S. Y. M. Chooi, P. Leung, S. Ng, G. H. Quek and K. Y. Sim, Tetrahedron: Asymmetry, 1991, **2**, 981–982.

7 (a) F. Liu, G. Zhao, W. Cai, D. Xu and B. Zhao, Org. Biomol. Chem., 2018, **16**, 7498–7502; (b) M. Chandrasekhar, G. Sekar and V. K. Singh, Tetrahedron Lett., 2000, **41**, 10079–10083; (c) H. S. Chong, X. Sun, Y. Chen and M. Wang, Tetrahedron Lett., 2015, **56**, 946–948; (d) M. R. Monaco, B. Poladura, M. D. L. Bernardos, M. Leutzsch, R. Goddard and B. List, Angew. Chem., Int. Ed., 2014, **53**, 7063–7067; (e) S.-Z. Lin and T.-P. You, Synth. Commun., 2009, **39**, 4133–4138; (f) Z. Chai, P. J. Yang, H. Zhang, S. Wang and G. Yang, Angew. Chem., Int. Ed., 2017, **56**, 650–654; (g) Y. H. Cho, V. Zunic, H. Senboku, M. Olsen and M. Lautens, J. Am. Chem. Soc., 2006, **128**, 6837–6846; (h) N. Taniguchi, T. Hata and M. Uemura, Angew. Chem., Int. Ed., 1999, **38**, 1232–1235.

8 (a) F. Orsini, G. Sello and G. Bestetti, Tetrahedron: Asymmetry, 2001, **12**, 2961–2969; (b) S. H. Jung and H. Kohn, J. Am. Chem. Soc., 1985, **107**, 2931–2943; (c) R. Annunziata, M. Benaglia, M. Caporale and L. Raimondi, Tetrahedron: Asymmetry, 2002, **13**, 2727–2734; (d) D. Yuan, Q. Peng, W. Xia, W. Yu,

L. Ruan, Y. Wang, Y. Chen and X. Pan, *Org. Process Res. Dev.*, 2024, **28**, 2623–2634.

9 (*a*) D. Chen, G. Xu, Q. Zhou, L. W. Chung and W. Tang, *J. Am. Chem. Soc.*, 2017, **139**, 9767–9770; (*b*) M. Zhou, K. Li, D. Chen, R. Xu, G. Xu and W. Tang, *J. Am. Chem. Soc.*, 2020, **142**, 10337–10342; (*c*) M. Zhou, Y. Lin, X.-X. Chen, G. Xu, L. W. Chung and W. Tang, *Angew. Chem., Int. Ed.*, 2023, **62**, e202300334; (*d*) Y. Lin, G. Xu and W. Tang, *J. Am. Chem. Soc.*, 2024, **146**, 27736–27744.

10 J. O. Hawthorne, E. L. Mhielic, M. S. Morgan and M. H. Wilt, *J. Org. Chem.*, 1963, **28**, 2831–2835.

11 (*a*) See ESI† for the computational details.; (*b*) Y. Zhao and D. G. Truhlar, *Theor. Chem. Acc.*, 2008, **120**, 215–241; (*c*) A. V. Marenich, C. J. Cramer and D. G. Truhlar, *J. Phys. Chem. B*, 2009, **113**, 6378–6396; (*d*) G. Luchini, J. V. Alegre-Requena, I. Funes-Ardoiz and R. S. Paton, *F1000 Research*, 2020, **9**, 291–305; (*e*) Q. Zhou, W. Tang and L. W. Chung, *J. Organomet. Chem.*, 2018, **864**, 97–104; (*f*) J. Lan, X. Li, Y. Yang, X. Zhang and L. W. Chung, *Acc. Chem. Res.*, 2022, **55**, 1109–1123; (*g*) Z. Ding, Z. Liu, Z. Wang, T. Yu, M. Xu, J. Wen, K. Yang, H. Zhang, L. Xu and P. Li, *J. Am. Chem. Soc.*, 2022, **144**, 8870–8882; (*h*) J. Cao, G. Wang, L. Gao, X. Cheng and S. Li, *Chem. Sci.*, 2018, **9**, 3664–3671; (*i*) L. Zhang and L. Jiao, *Chem. Sci.*, 2018, **9**, 2711–2722; (*j*) J. Liu, M. Nie, Q. Zhou, L. W. Chung, W. Tang and K. Ding, *Chem. Sci.*, 2017, **8**, 5161–5165; (*k*) J. L. Koniarczyk, J. W. Greenwood, J. V. Alegre-Requena, R. S. Paton and A. McNally, *Angew. Chem., Int. Ed.*, 2019, **58**, 14882–14886.

12 (*a*) S. Nagase and K. Morokuma, *J. Am. Chem. Soc.*, 1978, **100**, 1666–1672; (*b*) D. H. Ess and K. N. Houk, *J. Am. Chem. Soc.*, 2007, **129**, 10646–10647; (*c*) F. M. Bickelhaupt and K. N. Houk, *Angew. Chem., Int. Ed.*, 2017, **56**, 10070–10086; (*d*) I. Fernández and F. M. Bickelhaupt, *Chem. Soc. Rev.*, 2014, **43**, 4953–4967.

13 Z. Yan, Y. S. Liao, X. Li and L. W. Chung, *Chem. Sci.*, 2025, **16**, 2351–2362.

14 H. Vμzquez-Villa, S. Reber, M. A. Ariger and E. M. Carreira, *Angew. Chem., Int. Ed.*, 2011, **50**, 8979–8981.